Materials Science-Poland, *Vol. 26*, *No. 2*, *2008*

Structural and textural evolution of zirconia nanocrystals induced by thermal treatment

A. ADAMSKI[1*], P. JAKUBUS[2], Z. SOJKA[1, 3]

[1]Jagiellonian University, Faculty of Chemistry, ul. Ingardena 3, 30-060 Cracow, Poland

[2] Szczecin University of Technology, Institute of Chemistry and Environment Protection, al. Piastów 42, 71-065 Szczecin, Poland

[3]Regional Laboratory of Physicochemical Analyses and Structural Research, ul. Ingardena 3, 30-060 Cracow, Poland

Nanometric tetragonal and monoclinic zirconia was synthesized from zirconyl chloride by the modified forced hydrolysis method. Phase transitions and morphological changes accompanying zirconia calcination in the temperaure range 600–1000 °C were studied by XRD, HR-TEM techniques and N_2-porosimetry. Ageing of the amorphous hydrous zirconia at 100 °C for 48 h in the mother solution and its subsequent calcination at 600 °C for 6 h strongly favoured formation of single-phase tetragonal ZrO_2 of the thermal stability enhanced by 250 °C. Influence of the calcination temperature on phase composition, grain size, grain boundaries and pore structure of the resultant ZrO_2 material was analyzed.

Key words: *nanostructured ZrO_2; polymorphism; thermal evolution; grain size*

1. Introduction

Growing importance of nanosized zirconium dioxide in various practical applications is strongly related to its uniqe structural and physicochemical properties which remain decisive also for designing smart materials, tailored specifically to satisfy particular industrial needs. The most spectacular applications of ZrO_2 and related systems include ceramics, piezoelectrics, refractories, pigments, solid electrolytes and oxygen sensors [1, 2]. After morphological, textural and chemical valorization such materials can also be used in catalysis as active phases or supports [3, 4]. Many zirconia applications require high surface area development which should remain stable under process conditions. In the case of ZrO_2, structural and textural properties are strongly related to

*Corresponding author, e-mail: adamski@chemia.uj.edu.pl

its specific polymorphism. The crystalline structures of three ZrO_2 polymorphs such as low-temperature monoclinic ($P2_1/c$), high-temperature tetragonal ($P4_2/nmc$) and cubic ($Fm3m$) ones have been extensively studied [5, 6], however the extension of temperature windows of the occurrence of the two high-temperature phases is still a subject of research. These polymorphs cannot simply be quenched to room temperature, because they spontaneously undergo a martensic transition to the monoclinic form. They can, however, be effectively metastabilized by an appropriate bulk doping [4] or by controlling the size of particles [7]. Metastable phases are considered to be much more useful in many practical applications. Their principal advantages are related to a higher surface area and better developed pore structure. Therefore, an optimization of preparation procedure, leading to a desired form of zirconium oxide remains very often a vital necessity. A common route for preparation of zirconia consists in precipitation of a hydrous gel from aqueous solutions of a precursor salt and subsequent calcination of the amorphous precipitate. Short range ordering of oligomeric species formed in the parent solution containing fresh zirconia gel determines the spatial structure of the molecular framework, playing the role of a matrix for the topotactic crystallization of zirconia in a particular polymorph [8, 9]. Very important in this context is the role of ageing. Phase-oriented ZrO_2 synthesis should, however, include not only the control of parameters influencing zirconia proto-structures in aqueous solutions, but also of those which remain important during subsequent solid state changes accompanying thermal treatment.

The processes occurring during zirconia precipitation have already been discussed elsewhere [10]. In the present paper, influence of thermal treatment on the phase composition, crystal growth, and the textural properties of the resultant zirconium oxide will be analyzed based on the XRD and HR-TEM results, completed with N_2-porosimetry.

2. Experimental

Hydrous zirconia samples were obtained by the forced hydrolysis method from 0.6 M aqueous solutions of $ZrOCl_2 \cdot 8H_2O$ (Aldrich 99.99 %) with 25% ammonia at temperatures ranging from ambient temperature to 100 °C. Wet precipitate was washed with dilute NH_4NO_3 solution until negative test for Cl^- ions, and then divided into two parts. The first part was aged in the mother liquor (at pH ≈ 9) at 100 °C for 48 h under reflux and at the periodical supplementation of $NH_{3(aq)}$, then dried at 100 °C for 24 h, and calcined in air at 600 °C for 6 h. The other part was not subject to ageing, separated from the parent solution, dried and subsequently calcined in the same conditions.

X-ray diffraction patterns of the dried and calcined samples were recorded with the DRON-3 diffractometer (Bourevestnik, Russia) equipped with an iron filter, using

CuK_α and CoK_α radiations. The phase composition of the samples was calculated from the following equations:

$$X_t = \frac{I_t(111)}{I_t(111) + I_m(111) + I_m(11\bar{1})} \quad \text{and} \quad X_m = 1 - X_t \tag{1}$$

where X_t and X_m stand for the fractions of the tetragonal and the monoclinic forms, respectively, whereas I_t and I_m are the intensities of their diagnostic peaks [4]. The grain size was evaluated based on the Scherrer equation [11]

$$D_{hkl} = \frac{K\lambda}{B_{hkl}\cos\theta} \tag{2}$$

where λ stands for wavelength of the incident X-ray, B for the full width at the half maximum, θ is the corresponding Bragg angle and K is a constant

$$K = 2(\ln(2/\pi))^{1/2} = 0.93$$

For variable-temperature XRD experiments (VT-XRD), the samples were not pre-calcined but only dried and then heated stepwise to 1200 °C. At each 100 °C step an XRD pattern was recorded.

High resolution transmission electron microscopy (HR-TEM) was carried out using a JEM-100CX II UHR instrument (JEOL) operating at 100 kV. The specimens were prepared by deposition of the samples, ultrasonically dispersed in ethanol, on a holey carbon film supported on a copper grid.

3. Results and discussion

A distinct difference exists in structural response to increase of temperature between ZrO_2 samples prepared by conventional precipitation from aqueous solutions, i.e., without ageing, and those subject to ageing in the mother liquid at 100 °C for 48 h. As revealed by the results of VT-XRD experiments, cristallization of the amorphous non-aged hydrous zirconia occurs between 300 °C and 400 °C. In the XRD pattern recorded at 400 °C, a strong single line attributed to the (111) reflection of the tetragonal phase appeared in the diagnostic 2θ region between 25° and 33° for CuK_α radiation (or 31° and 38° for CoK_α radiation) [4] (Fig.1). Low-temperature tetragonal polymorph is a metastable phase, appearing in variable concentration in zirconia prepared by precipitation. In our case, it was the only phase existing in the temperature range of 400–600 °C. The next phase transition, related to the transformation of the metastable tetragonal ZrO_2 to the thermodynamically stable monoclinic one, occurred between 600 °C and 700 °C. In the XRD pattern recorded at 700 °C, a distinct line due to the $(11\bar{1})$ reflection and a broadening of the (111) reflection appeared, being diag-

nostic of the monoclinic phase. Both polymorphs coexisted in the temperature range of 700–800 °C but the contribution of t-ZrO_2, equal to $X_t \approx 71.5\%$ at 700 °C decreased upon temperature increase, reaching zero after annealing of the samples at 900 °C. For the aged samples, temperatures of both phase transitions are shifted up by at least 100 °C, as can be seen in Fig. 1. Aged $ZrO_2 \cdot xH_2O$ crystallized between 400 °C and 500 °C in the tetragonal form and weak Bragg maxima from m-ZrO_2 appeared at first at 1000 °C. Disappearence of t-ZrO_2 has a drastic negative effect on the specific surface area of ZrO_2 materials (around 47% decrease). Fortunately for zirconia applications as a support, the temperature window of existence of the metastable t-ZrO_2 is expanded by 200 °C for aged samples in comparison to the non-aged ones.

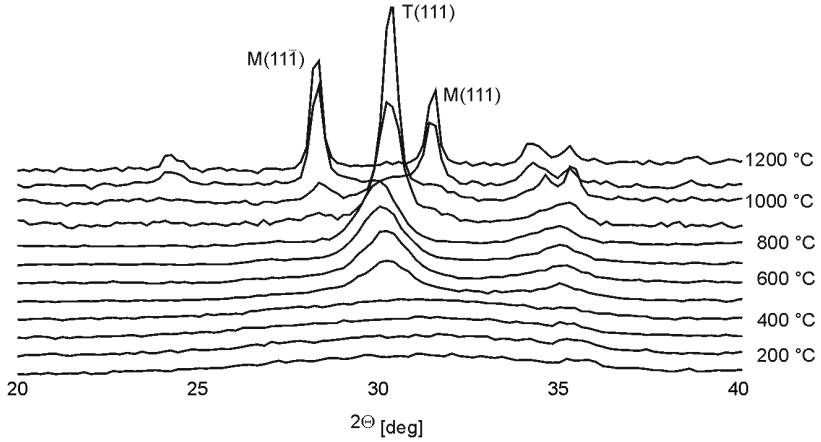

Fig. 1. Variable temperature XRD patterns (VT-XRD) for hydrous zirconia aged in the mother solution at 100 °C for 48 h

The observed differences in temperature of crystalization and in thermal decay of t-ZrO_2 clearly reflect differences in grain sizes and degrees of their agglomeration between non-aged and aged zirconia. It is noteworthy that the particle sizes of both polymorphs coexisting at 800 °C, evaluated based on Eq. (2), were always distinctly higher for the non-aged samples (D_t = 28.2 nm, D_m = 56.3 nm) in comparison to those obtained for aged preparations (D_t = 8.7 nm, D_m = 39.2 nm). Simultaneously, in both cases D_m was higher than the critical particle size for the tetragonal to monoclinic transformation, reported in the literature to be equal to 30 nm [7]. Simultaneously, as revealed by TEM images of the non-aged samples, the particles were strongly agglomerated forming a hard compact, whereas in the case of aged materials the particles were loosely arranged, preserving their distinct shape giving rise to microporosity development, observed in N_2-sorption experiments.

Particle size and the nature of the grain boundaries are thus the primary factors controlling metastabilization of t-ZrO_2. They can be modified by both ageing and the calcination temperature, allowing effective controlling of the t-ZrO_2/m-ZrO_2 ratio. Figure 2 shows the dependences of the content of t-ZrO_2 phase on crystallite size eva-

luated from Eq. (2) for the aged (curve a) and non-aged (curve b) zirconia, heated in the temperature range 400–900 °C.

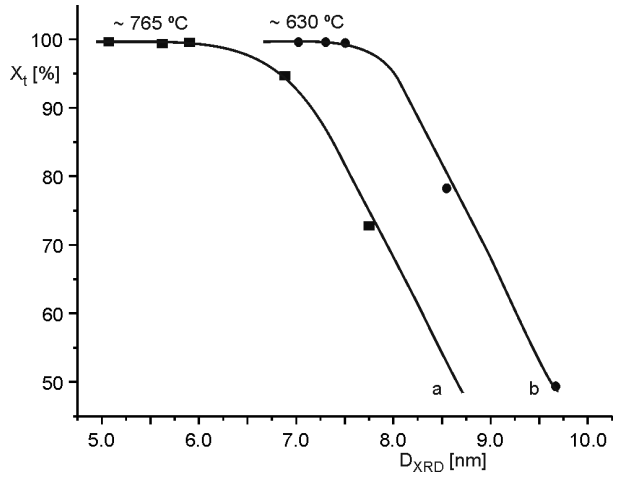

Fig. 2. Particle-size dependent changes in the *t*-ZrO_2 content in the aged (a) and non-aged (b) samples, calculated from XRD data recorded in the temperature range 400–900 °C

The content of *t*-ZrO_2 phase remained constant until d = 7.0 nm and 8.5 nm for aged and non-aged samples, respectively, i.e. below the threshold particle size for metastabilization of the tetragonal ZrO_2 [7]. Then it severely decreased as the particle size increased due to rapid sintering caused by migration of grain boundaries. If the process of destabilization of the low-temperature *t*-ZrO_2 phase by its transformation into *m*-ZrO_2 is governed mainly by the thermodynamic properties, then neglecting the strain difference between *t*- and *m*-ZrO_2 crystals, the inequality should be fulfilled:

$$(G_m + \gamma_m S_m) - (G_t + \gamma_t S_t) < 0 \tag{3}$$

where G stands for the molar free enthalpy, γ for the surface energy and S for the surface area of the monoclinic and tetragonal phases [7]. The term $(G_m - G_t)$ is negative at room temperature (–4.73 kJ/mol [7]), thus to preserve the *t*-ZrO_2 polymorph, the term $(\gamma_m S_m - \gamma_t S_t)$ should be positive and higher than the difference in the free enthalpies. Taking into account anomalous excess of the surface energy of the monoclinic phase (γ_m = 1.13 J/m^2) in comparison to the tetragonal one (γ_t = 0.77 J/m^2) [12], the sign of the term $(\gamma_m S_m - \gamma_t S_t)$ depends on the surface area, which, within the spherical shape approximation, is closely related to the particle size following the equation:

$$S = \frac{6 \times 10^3}{D_{BET}\rho} \tag{4}$$

where ρ stands for the density of a given phase and D_{BET} is the particle size (in nm). The results of our porosimetric measurements, performed for non-aged and aged zir-

conia samples calcined at 600 °C for 6 h, revealed that the surface area in the case of aged zirconia, S = 77.05 m^2/g is almost 3.5 times higher than that of the non-aged sample (23.28 m^2/g) [13]. Because the aged samples were purely tetragonal at 600 °C, the particle size determined from Eq. (4) using ρ_t = 6.10 g/cm^3 was equal to D_{BET} ≈ 12.7 nm, being in a nice agreement with D_{hkl} = 11.2 nm obtained from the XRD data. This finding indicates that the entire surface is accessible for the adsorbate which is in line with the loose structure of the nanopowder observed in TEM. Thus the digestion of the hydrous zirconia in the mother liquid leads to a fine-grained ZrO_2 of well developed porosity, which is more resistant to the sintering as the temperature increases and remains tetragonal over a wider temperature range. The non-aged, agglomerated zirconia is more susceptible to the transformation into monophase *m*-ZrO_2. The influence of ageing on the morphology and metastablization of *t*-ZrO_2 was discussed elsewhere [10].

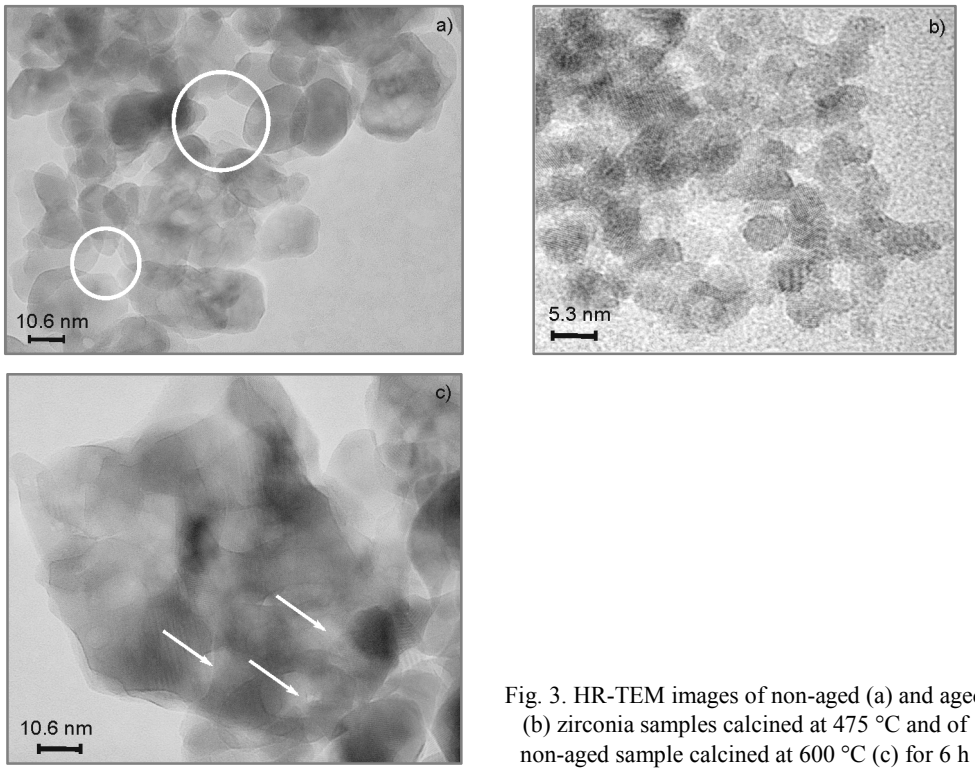

Fig. 3. HR-TEM images of non-aged (a) and aged (b) zirconia samples calcined at 475 °C and of non-aged sample calcined at 600 °C (c) for 6 h

As already mentioned, temperature increase results not only in changes in particle sizes but also in their shape. HR-TEM images taken for non-aged zirconia samples calcined at 475°C for 24 h show numerous crystallites of a distinct size and shape variety, typical of *t*- and *m*-ZrO_2 mixtures (Fig. 3a). Inspection of the corresponding XRD pattern confirmed the presence of both polymorphs. In majority, the crystallites are oval, elongated with one or two slightly marked facets. Smaller, isolated particles

of ca. 17–25 nm in diameter are accompanied by several more sintered larger grains of 34–40 nm. Very characteristic is a tendency of non-aged ZrO_2 particles to agglomerate in crown-like structures which are marked with white circles in Fig. 3a. HR-TEM micrographs for aged zirconia samples calcined in the same conditions (Fig. 3b) revealed the presence of distincly smaller non-agglomerated crystallites, typical of *t*-ZrO_2, generally not exceeding 6 nm. The crystallites are more oval, relatively well separated and loosely arranged. High-resolution images for samples calcined at 600 °C show distinct effects caused by temperature increase which are much more pronounced for non-aged zirconia. The arrangement of crystallites is distinctly denser in comparison to that observed after zirconia calcination at 475 °C, with very few partially or completely filled crown-like structures which appear in some favourable cases and are marked with arrows in Fig. 3c. Parallel XRD patterns indicate the presence of *m*-ZrO_2 as a majority polymorph. Crystallites are large, of diameters often exceeding 80–100 nm and rectangular shapes. The grain boundaries are favoured over free surface, and the interparticle coordination number increases. Contrary to this, the crystallites of aged ZrO_2 remain separated and do not exceed 7–17 nm in size (Fig. 4). The voids between the grains are well pronounced accounting for relatively well developed micro- and mesoporosity, characteristic of the *t*-ZrO_2 samples [13, 14].

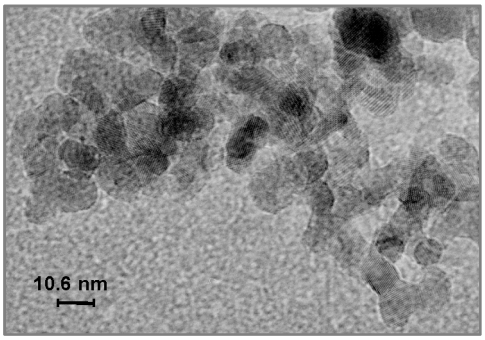

Fig. 4. HR-TEM image of aged zirconia sample calcined at 600 °C for 6 h

4. Conclusions

Ageing and thermal treatment are the most important synthetic steps of zirconia preparation, decisive for controlling the *t*-ZrO_2/*m*-ZrO_2 ratio. Prolonged digestion of the zirconia precipitate in the mother liquor at 100 °C allows effective controlling of the zirconia grain size and grain boundaries, resulting in expansion of the thermal stability of the *t*-ZrO_2 polymorph.

Acknowledgements

This work was financially supported by The Polish State Committee for Scientific Research (KBN) within the project No. 3 T09 147 26.

References

[1] LEE J.-H., J. Mater. Sci., 38 (2003), 4247.
[2] RAINFORTH W.M., J. Mater. Sci., 39 (2004), 6705.
[3] YAMAGUCHI T., Catal. Today, 20 (1994), 199.
[4] MERCERA P.D.L., VAN OMMEN J.G., DOESBURG E.B.M., BURGGRAAF A.J., ROSS J.R.H., Appl. Catal. 57 (1990), 127.
[5] WELLS A.F., *Structural Inorganic Chemistry*, Polish Ed., WNiT, Warsaw, 1993.
[6] JUNG K.T., BELL A.T., J. Mol. Catal. A, 163 (2000), 27.
[7] GARVIE R.C., J. Phys. Chem., 69 (1965), 1238.
[8] CHEN S.-G., YIN Y.-S., WANG D.-P., J. Mol. Struct., 690 (2004), 181.
[9] TANI E., YOSHIMURA M., SŌMYIA S., J. Am. Ceram. Soc., 66 (1983), 11.
[10] ADAMSKI A., JAKUBUS P., SOJKA Z., Nukleonika 51 (Suppl. 1) (2006), S27.
[11] PATTERSON A.L., Phys. Rev., 56 (1939), 978.
[12] CHRASKA T., KING A.H., BERNDT CH.C., Mat. Sci. Eng. A, 286 (2000), 169.
[13] JAKUBUS P., ADAMSKI A., KURZAWA M., SOJKA Z., J. Therm. Anal. Calorim., 72 (2003) 299.
[14] ADAMSKI A., JAKUBUS P., SOJKA Z., Solid State Phenom., 128 (2007), 89.

Received 28 April 2007
Revised 16 February 2008